Optical constants of ice from the ultraviolet to the microwave: A revised compilation

Stephen G. Warren[1] and Richard E. Brandt[1]

[1] A compilation of the spectral absorption coefficient of ice Ih is presented for temperatures near the melting point, superseding the compilation of Warren (1984). Significant changes are made to nearly all spectral regions. The blue and near-ultraviolet absorption is much weaker than the prior estimates, which were already very small. The near-infrared absorption coefficient differs by as much as a factor of 2 from the prior compilation at some wavelengths. The midinfrared absorption coefficient is rather uncertain in the weakly absorbing regions near 9 and 20 μm. New far-infrared measurements at low temperatures are extrapolated to higher temperatures, which shifts the peak positions. New microwave measurements find absorption much weaker than previously reported, by factors of 2–5. The real part of the index of refraction is computed using Kramers-Kronig analysis; it differs from the prior compilation only in the far infrared. Tables of the revised optical constants are available on a website.

Citation: Warren, S. G., and R. E. Brandt (2008), Optical constants of ice from the ultraviolet to the microwave: A revised compilation, *J. Geophys. Res.*, *113*, D14220, doi:10.1029/2007JD009744.

1. Introduction

[2] *Warren* [1984] (hereinafter referred to as W84) reviewed measurements of the absorption coefficient and refractive index of ordinary hexagonal ice Ih, and compiled a set of recommended values of the optical constants. The optical constants are needed for understanding radiative properties of ice and ice-containing media such as snow and clouds, with applications to energy budgets and remote sensing. The 1984 compilation is still in use more than 20 years later, but in the meantime more accurate measurements have been made in many parts of the spectrum. Therefore, we have prepared a revised compilation. Depending on the application and the spectral region of interest, the differences from the 1984 compilation may or may not be significant. (The revised compilation is available as tables at http://www.atmos.washington.edu/ice_optical_constants.)
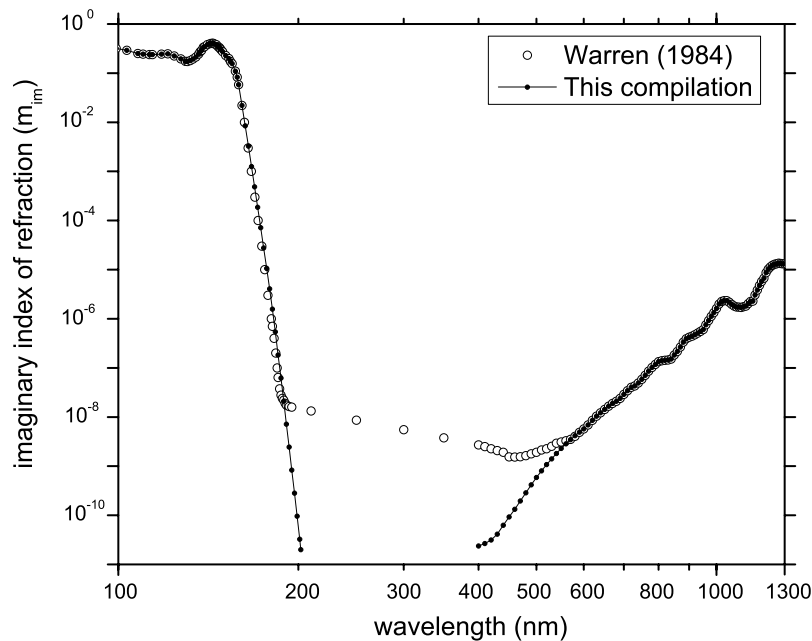
[3] We report the complex index of refraction, $m = m_{re} + i\, m_{im}$, as a function of wavelength λ, where m_{im} is related to the linear absorption coefficient k_a, as $k_a = 4\pi m_{im}/\lambda$. The values we tabulate are appropriate for ice Ih at temperatures not far below the melting point; they are given for a nominal temperature $T = 266$ K. Some of the measurements we cite were made at lower temperatures for application to planets colder than Earth. Those references can be consulted for low-temperature applications. *Woschnagg and Price* [2001] reviewed experimental results from several publica-

tions and concluded that the absorption coefficient of ice increases with temperature by approximately 1% K^{-1} for all weakly absorbing parts of the spectrum from the UV (175 nm) to the microwave (1 cm). This result was confirmed for the millimeter wave region by *Zhang et al.* [2001]. However, temperature dependence increases rapidly with wavelength beyond 1 cm. In some spectral regions the temperature dependence has been measured only at very low temperatures, so we are reluctant to use it to alter values of measurements made near the melting point. Also, in some spectral regions there are deviations from the Woschnagg-Price rule. Therefore, where measurements were made within 20 K of our nominal temperature of 266 K, we simply accept the values as reported. Here we summarize our choices of data sources and our procedures for connecting them.

2. Visible and Near Visible Regions (160–1400 nm)

[4] For wavelengths 600–1400 nm we continue to use the measurements of *Grenfell and Perovich* [1981] (hereinafter referred to as GP); they are accurate in this wavelength domain and have not been superseded. At shorter wavelengths, 250–600 nm, the laboratory transmission measurements of GP and *Perovich and Govoni* [1991] were called into question by measurements of the Antarctic Muon and Neutrino Detector Array (AMANDA). AMANDA measured the frequency distribution of photon travel times from a pulsed source in clear glacier ice deep in the Antarctic ice sheet at the South Pole, over distances up to 200 m [*Ackermann et al.*, 2006]. The frequency distribution of travel times can be fitted by a function with two coefficients:

[1]Department of Atmospheric Sciences, University of Washington, Seattle, Washington, USA.

Figure 1. Imaginary part of the complex index of refraction of ice in the ultraviolet and visible region; comparison of the new compilation to that of *Warren* [1984].

the scattering coefficient k_s and the absorption coefficient k_a. The values of k_a inferred by AMANDA were lower than those obtained from the laboratory measurements, by more than an order of magnitude at $\lambda = 400$ nm, indicating that the attenuation in the laboratory measurements, which had been attributed to absorption, had partly been caused by scattering. The contribution of scattering became dominant in the wavelength region of minimum absorption near 400 nm. Because of dust naturally present in the Antarctic ice, in amounts which vary through ice age cycles, the values of k_a obtained by AMANDA are upper limits for k_a of pure ice.

[5] AMANDA's low values of k_a were confirmed by measurements of spectral transmission of sunlight into Antarctic surface snow [*Warren et al.*, 2006] (hereinafter referred to as WBG). Snow is a scattering-dominated medium whose scattering coefficient is independent of wavelength across the visible and near ultraviolet. The attenuation of solar radiation in snow can be used to infer k_a by reference to the known value at 600 nm (where GP and AMANDA were in agreement). WBG developed this method and derived values of k_a for wavelengths 350–600 nm. The minimum absorption is found at $\lambda_{\min} =$ 390 nm in agreement with AMANDA, as compared to $\lambda_{\min} = 470$ nm reported by GP (and used by W84). The value of k_a at 390 nm inferred by WBG is lower than even the lowest values of AMANDA by a factor of 6.

[6] Absorption by ice is extremely weak at $\lambda = 390$ nm, and the measured absorption at that wavelength was probably dominated by trace impurities both in the snow of WBG and in the ice of AMANDA. Therefore, we cannot be sure where the absorption minimum actually occurs for pure ice. Analyses by *He and Price* [1998, Figure 1] and *Askebjer et al.* [1997, Figure 9] suggest that the wavelength of minimum absorption for pure ice is located between 200 and 300 nm. Therefore, we use the data of WBG from 600 nm down to 390 nm, where k_a reaches its minimum measured value ($m_{im} = 2 \times 10^{-11}$). We leave a gap in the

compilation between 200 and 390 nm (Figure 1). In this domain, $m_{im} \leq 2 \times 10^{-11}$. For most applications this extremely low value of m_{im}, indicating an absorption length $k_a^{-1} = 1.5$ km at $\lambda = 390$ nm, will be indistinguishable from zero.

[7] The steep rise of m_{im} in the "Urbach tail" of the ultraviolet absorption, from 200 to 160 nm, has also been revised. The extinction coefficients reported by *Minton* [1971] for 181–185 nm had been defined on base-10 but were misinterpreted by W84 as extinction coefficients on base-e. We now use the corrected values; we connect Minton's 181-nm value to W84's 161-nm value using a linear interpolation of log k_a versus λ, which is the wavelength dependence expected for the Urbach tail [*He and Price*, 1998]. We extrapolate Minton's data downward to $\lambda =$ 202 nm, where m_{im} matches the lowest value of WBG (at 390 nm). Between 202 and 390 nm we just report $m_{im} \leq 2 \times 10^{-11}$, as indicated above. For the strongly absorbing UV wavelengths, $\lambda < 160$ nm, our compilation is unchanged from that of W84. Figure 1 compares our new compilation to the 1984 compilation for wavelengths 100–1300 nm.

3. Near Infrared Region (1.4–7.8 μm)

[8] We have revised the entire wavelength region 1.4–7.8 μm except for the 3-μm absorption band. This region has been studied by *Rajaram et al.* [2001], who made measurements at temperatures 166–196 K and also thoroughly reviewed measurements at higher temperatures by other authors. We accept the judgments of Rajaram et al. for most of this spectral region. For the 3-μm band we continue to recommend the measurements at 266 K by *Schaaf and Williams* [1973] (hereinafter referred to as SW), which had been adopted by W84 for 2.8–33 μm. SW used a reflection method, which is appropriate for regions of strong absorption.

[9] *Gosse et al.* [1995] (hereinafter referred to as GLC) measured transmission from 1.4 to 7.8 μm at $T = 251$ K,
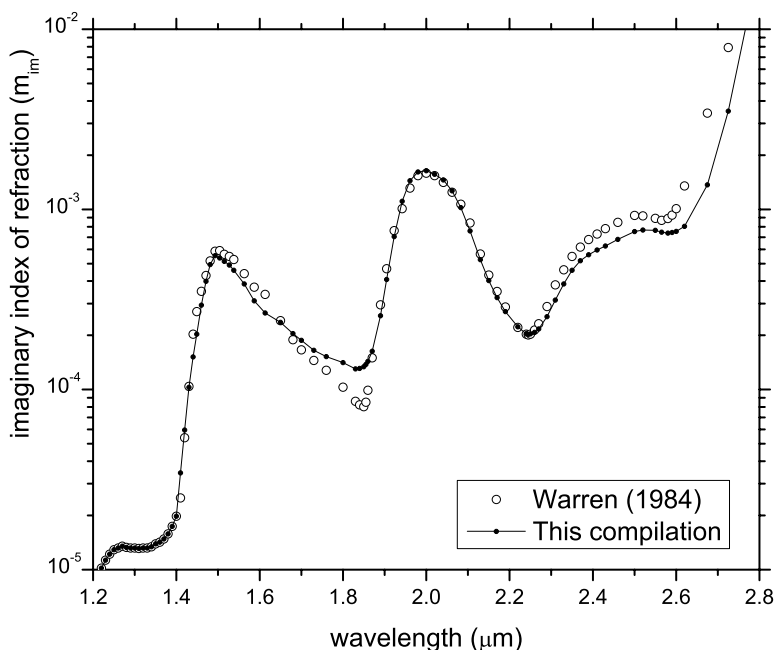
Figure 2. Imaginary part of the complex index of refraction of ice in the near infrared, $1.2-2.8$ μm; comparison of the new compilation to that of *Warren* [1984].

which agreed with earlier measurements in the same laboratory by *Kou et al.* [1993] where they overlapped. GLC were able to obtain m_{im} accurately in regions of weak absorption but not in the strong 3-μm band, so their values complement the reflectance measurements of SW. *Grundy and Schmitt* [1998] (hereinafter referred to as GS) also measured transmission, at several temperatures between 20 and 270 K, for wavelengths $1.0-2.7$ μm.

[10] For most of the region $1.4-2.1$ μm, W84 had used the measurements of *Ockman* [1957, 1958]. *Rajaram et al.* [2001] reanalyzed Ockman's data, properly accounting for reflections at the interfaces of a thin film. That result agreed better with GLC than with GS, causing Rajaram et al. to favor the GLC values; we adhere to that choice. However, the GS values differ only slightly from the GLC values. We use GLC for $1.4-7.8$ μm, except for the 3-μm band. Comparing Rajaram et al. (196 K) and GLC (250 K) at $\lambda = 2.65$ μm, we infer $dk_a/dT = 0.6\%$ K^{-1}, in rough agreement with *Woschnagg and Price*'s [2001] estimate of 1% K^{-1}. However, at longer wavelengths, $7-8$ μm, the k_a of *Toon et al.* [1994] at 163 K agrees with that of GLC at 250 K, indicating no temperature dependence. This result contrasts with the estimate of $dk_a/dT = 1\%$ K^{-1} inferred by *Woschnagg and Price* [2001] from measurements of *Maldoni et al.* [1998] for temperatures $120-140$ K, suggesting that dk_a/dT may itself vary with temperature.

[11] In summary, the new compilation uses GLC for $1.4-2.9$ μm, SW (same as W84) for the 3-μm band ($2.9-3.4$ μm), and GLC for $3.4-7.8$ μm. This region of the spectrum is plotted in Figures 2 and 3.

## 4. Middle and Far Infrared Regions ($7.8-200$ μm)

[12] In this spectral region ice is strongly absorbing. New measurements have been made but only at low temperatures. Many of the new measurements are for cubic ice or

amorphous ice rather than hexagonal ice. This spectral region is of great interest for planetary astronomy. Measurements were made at temperatures $77-150$ K for wavelengths $20-200$ μm by *Johnson and Atreya* [1996], at $13-155$ K for $20-100$ μm by *Moore and Hudson* [1992], at $10-140$ K for $2.5-25$ μm (strong bands only) by *Maldoni et al.* [1998], and at $106-176$ K for $15-200$ μm by *Curtis et al.* [2005].

[13] A thorough study for $1.4-20$ μm at $T < 200$ K was carried out for ice, as well as for complexes of ice with nitric acid, by *Toon et al.* [1994] for application to polar stratospheric clouds. In the strong absorption bands at 3 μm and 12 μm their values deviate from those of SW, probably because both the strengths and locations of the strong bands depend on temperature. For these strong bands we therefore continue to recommend the measurements of SW because they were made at $T = 266$ K. SW measured reflection, which is sensitive to m_{im} only where m_{im} is large (comparable in magnitude to m_{re}), so their method is appropriate for the strong absorption bands.

4.1. Midinfrared Region ($7.8-26$ μm)

[14] Three data sets are available for the region surrounding the 12-μm libration band: transmission measurements by *Bertie et al.* [1969] (hereinafter referred to as BLW) at 100 K, reflection measurements by *Schaaf and Williams* [1973] at 266 K, and transmission measurements by *Toon et al.* [1994] (hereinafter referred to as T94) at 163 K. The values of T94 are shown in Figure 4, along with those of SW (which were used by W84 across this entire region). For $m_{im} > 0.1$ we favor the measurements of SW because they were made at the higher temperature. In the tails of the 12-μm band the reflection method of SW becomes inaccurate. For the region $8-10$ μm it is difficult to decide what to recommend. Both T94 and BLW show a minimum of m_{im} at 9.5 μm (Figure 4a of T94). They agree closely with each
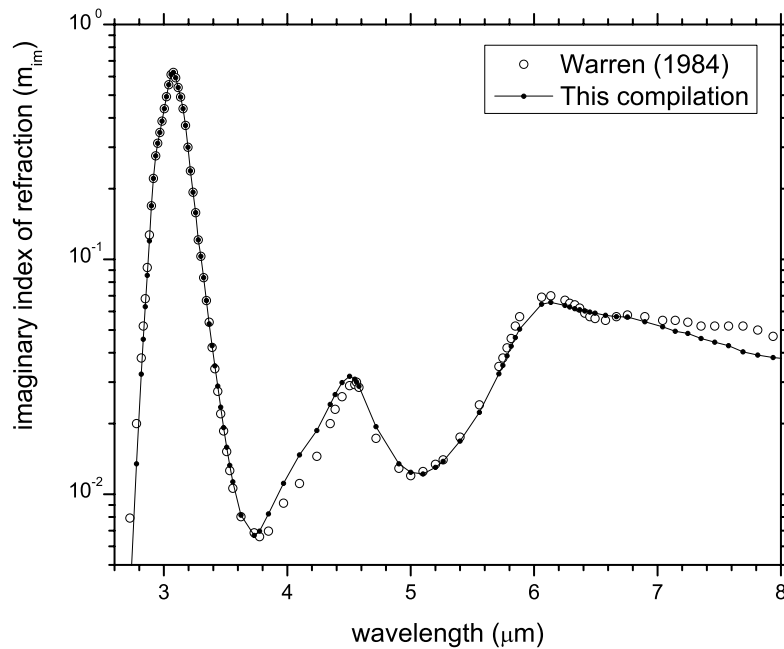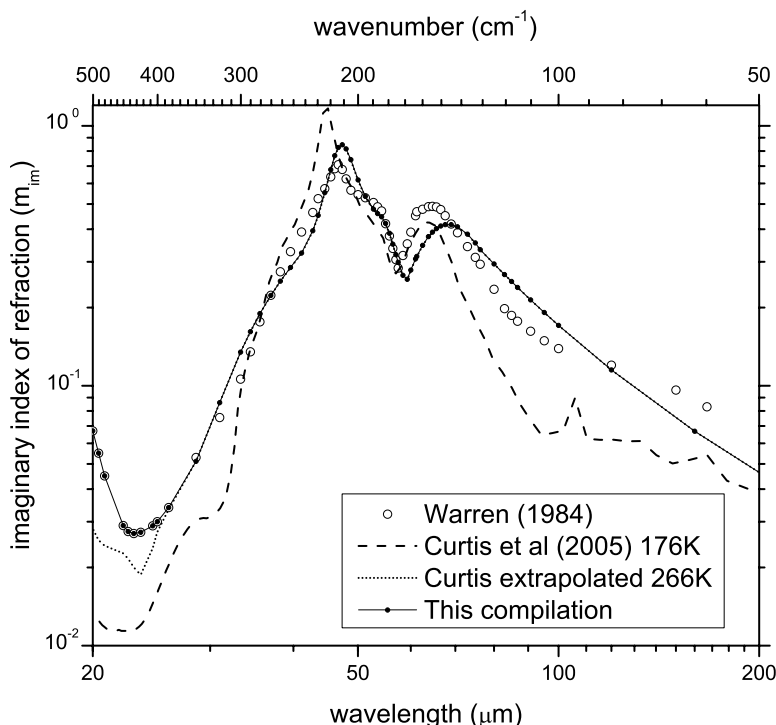
Figure 3. Imaginary part of the complex index of refraction of ice in the infrared, 2.7−8.0 μm; comparison of the new compilation to that of *Warren* [1984].

other and disagree with SW, who did not find this minimum. The agreement of BLW's measurements at 100 K with T94's at 163 K suggests that the temperature dependence is small near $\lambda = 9$ μm (it also was small at 7−8 μm as indicated in section 3). However, BLW did not account

for reflection at the interfaces in their derivation of m_{im} from thin-film transmission measurements, so their agreement with T94 may be fortuitous. The plots of *Tsujimoto et al.* [1982], who did account for reflection, do show m_{im} increasing with temperature at 9.5 μm, with m_{im} values
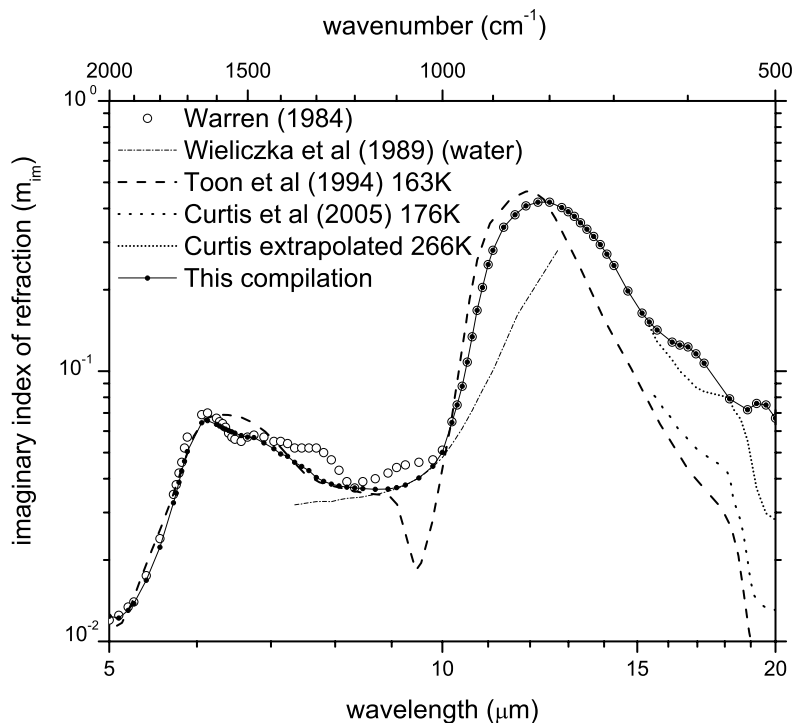
Figure 4. Imaginary part of the complex index of refraction of ice in the midinfrared, 5−20 μm (500−2000 cm^{-1}); comparison of the new compilation to the compilation of *Warren* [1984] and to the data of *Toon et al.* [1994] at 163 K. Data of *Curtis et al.* [2005] are shown as reported for 176 K and as extrapolated to 266 K. The values for liquid water are also shown from *Wieliczka et al.* [1989]. The compilation of *Warren* [1984] used *Schaaf and Williams* [1973] for this entire spectral region.

Figure 5. Imaginary part of the complex index of refraction of ice in the far infrared, $20-200$ μm ($50-500$ cm^{-1}); comparison of the new compilation to the compilation of *Warren* [1984] and to the data of *Curtis et al.* [2005]. *Warren* [1984] used *Schaaf and Williams* [1973] for $20-33$ μm.

approximately 0.014, 0.022, and 0.029, respectively, at temperatures 77, 150, and 180 K, indicating a temperature dependence not far from the 1% K^{-1} of *Woschnagg and Price* [2001]. The dip at 9.5 μm becomes less prominent as the temperature increases. The spectrum of liquid water, also plotted in Figure 4, does not show even a slight dip at 9.5 μm [*Wieliczka et al.*, 1989]. *Zimmermann and Pimentel* [1962, Figure 1] showed that amorphous ice at 93 K lacked the dip at 9.5 μm; the dip appeared when the amorphous ice was annealed to crystalline ice at 178 K. The spectrum of liquid water, therefore, resembles that of amorphous ice in this region. The warm ice of SW also lacks the dip, in spite of its crystalline nature.

[15] We have decided to continue to rely on SW's measurements in this region; this choice is supported by the filling in of the 9.5-μm dip with warming shown by *Tsujimoto et al.* [1982]. However, we think that SW's published error bars are too small. Figure 4 shows that the SW values wander about the smooth spectrum of GLC from 6 to 8 μm and are in error by as much as 30%. Therefore, rather than following every wiggle of SW, we use SW's data as a guide for drawing a smooth curve.

[16] For the compilation we note that GLC and T94 agree between 7 and 8 μm, and that T94 agrees with SW at 8.3 μm. We draw a smooth curve from 7.8 μm to meet SW's value at 10.3 μm, passing through SW's value at 8.3 μm where it agrees with T94. Between 9 and 10 μm our compilation is, therefore, intermediate between T94 and SW and may be considerably in error. We use SW's values exactly as reported beginning at 10.3 μm and across the 12-μm libration band.

[17] On the longwave side of the libration band, 15–26 μm, the temperature dependence of m_{im} is large, as

indicated by *Tsujimoto et al.* [1982]. T94 argued that SW's reported values of m_{im} were too large in the wavelength region 15–20 μm. But what T94 meant was that SW's values at 266 K could not explain T94's transmission measurements at 163 K. New measurements by *Curtis et al.* [2005] at temperatures 156–176 K can be used to estimate a temperature dependence in this region (described in detail in section 4.2). Extrapolating the Curtis et al. measurements to 266 K would give values not far from those of SW (Figures 4 and 5). But extrapolating by 90 K using a temperature dependence obtained over only a 20 K interval is unreliable, so we continue to use SW as our primary source for this region.

[18] The data points of SW (as reported by W84) are plotted in Figures 4 and 5. SW's data become more inaccurate toward their longwave end, with error bars on m_{im} of 0.03 at $\lambda = 33$ μm (SW Figure 4b), so we transition from SW to the temperature-adjusted values from *Curtis et al.* [2005] (described in section 4.2) at a point where they agree, $\lambda = 26$ μm. In summary, the new compilation (Figures 4 and 5) uses a hand-drawn curve intermediate between GLC and SW for 7.8 to 10.3 microns; from 10.3 to 26 microns the compilation uses SW.

4.2. Far Infrared Region (26–200 μm)

[19] The far-infrared region contains two strong absorptions near 45 and 65 μm, due to lattice vibrations in the hydrogen-bonded ice crystal. The measurements available to W84 for the far infrared were the thin-film transmission measurements of BLW at 100 K and of *Bertie and Whalley* [1967] (hereinafter referred to as BW) at 100 and 168 K. Those analyses did not account for reflection losses at the interfaces, which vary considerably with wavelength across

the two strong bands. BW had no measurement of sample thickness; BLW determined sample thickness by an indirect method.

[20] Those measurements have now been superseded by transmission measurements of *Curtis et al.* [2005] that were interpreted using Kramers-Kronig analysis, accounting for interface reflections and thin-film interference. The measurements were made at eight temperatures. At the three lowest temperatures (106, 116, and 126 K) the ice was amorphous, so we ignore those three spectra. At 136 K and above the ice was crystalline, either cubic ice Ic or hexagonal ice Ih or a mixture. However, the spectra of ice Ic and ice Ih are nearly identical in this spectral region. They were indistinguishable in the measurements of BW (Figure 3 of BW). *Bertie and Jacobs* [1977] did find a subtle difference between cubic and hexagonal ice at $160-170$ cm^{-1}, which *Curtis et al.* [2005] used to try to identify their samples: ice Ih at 176 K and probably ice Ic or mixtures of Ih and Ic at $136-166$ K. We use the data for the three highest temperatures (156, 166, and 176 K) from *Curtis et al.* [2005] to infer a temperature dependence that we can then extrapolate to 266 K. We ignore the data at the intermediate temperatures 136 and 146 K because they appear noisier crossing the higher-temperature curves. Our steps for determining a temperature extrapolation are as follows:

[21] 1. To the three plots of k_a versus wave number (ν) we fitted the following analytical functions: a Lorentzian curve for the 45-μm peak ($198-253$ cm^{-1}) and a Gaussian for the 65-μm peak ($102-175$ cm^{-1}). In the transition from 100 to 50 cm^{-1}, k_a appeared to ramp linearly downward; a linear fit of $k_a(\nu)$ was obtained from 91 to 52 cm^{-1} at each temperature.

[22] 2. The parameters of the fits (corresponding to height, width, peak wave number, and baseline) of $k_a(\nu)$ were extrapolated linearly in temperature to 266 K; then the three partial spectra $k_a(\nu)$ were computed (for the two absorption bands and the "100-μm ramp"). The temperature dependence of the 220-cm^{-1} peak has been discussed by *Schmitt et al.* [1998, Figure 7]. As temperature increases, the peak broadens, the peak intensity decreases, and the peak position shifts to longer wavelengths. This was also seen by *Curtis et al.* [2005], so our extrapolation of the Curtis et al. data continues these trends (Figure 5). For the shortwave end of the Curtis et al. data, $16-31$ μm, a linear temperature dependence was computed at each wavelength individually and extrapolated to 266 K. The resulting spectrum was smoothed using an eight-point running mean for $16-19$ μm and a five-point running mean for $19-31$ μm.

[23] 3. Each partial spectrum was joined to its neighbor with a cubic spline in log m_{im} versus log λ. The *Curtis et al.* [2005] data are noisy in the region $100-200$ μm (dashed line in Figure 5) because the absorption is becoming weaker approaching the noise level at 200 μm (50 cm^{-1}) as shown by *Curtis et al.* [2005, Figure 7b]. Therefore, we drew a smooth curve through this region, a cubic spline, connecting the Gaussian fit at $\lambda = 75$ μm to the microwave value at $\lambda = 300$ μm.

[24] 4. A Kramers-Kronig (KK) analysis (described in section 6) was done on the entire spectrum. As in W84, the strengths of the two far-IR absorptions were adjusted

so that the KK analysis produced the correct measured value of microwave m_{re} (section 6).

[25] The band strength, $\int k_a d\nu$, integrated over both lattice vibrations from 102 to 326 cm^{-1} ($30.7-98$ μm), varies by $\pm 3\%$ for the five temperatures of hexagonal ice, with no systematic temperature dependence. The extrapolated spectrum at 266 K, both before and after KK analysis and adjustment (see section 6), is also within this small range. The cubic spline we used from 75 to 300 μm was adjusted slightly to keep the band strength within this range.

[26] In summary, the new compilation uses the data of *Curtis et al.* [2005] (with our temperature adjustment) for wavelengths $26-200$ μm. The data are compared to the 1984 compilation in Figures 4 and 5.
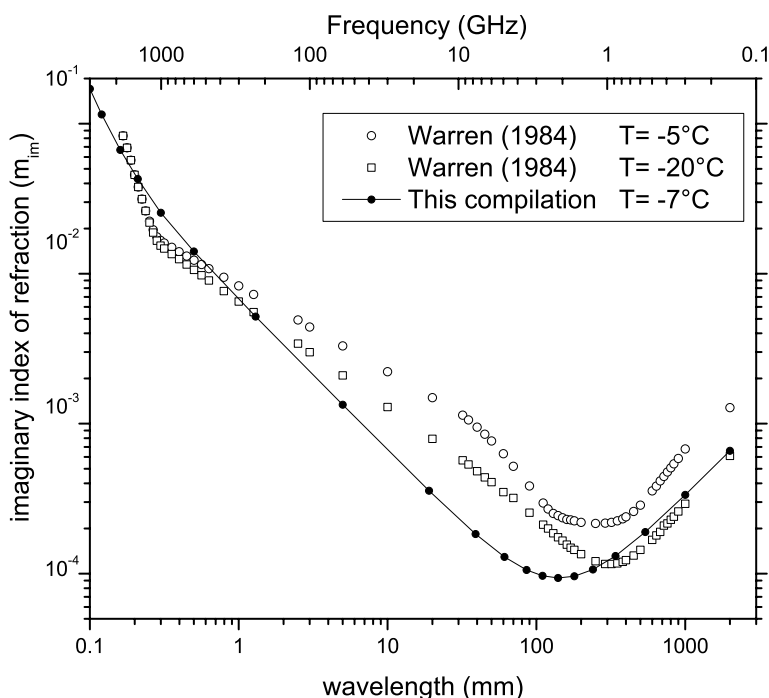
5. Microwave

[27] *Mätzler and Wegmüller* [1987] (hereinafter referred to as MW) measured dielectric loss for frequencies 2 to 100 GHz (wavelengths $3-150$ mm) at temperatures of 258 and 268 K. Subsequent measurements over the frequency range $5-39$ GHz (wavelengths $8-60$ mm) by *Matsuoka et al.* [1996] at several temperatures agreed with MW at the temperature they had in common (258 K). *Koh* [1997] found a "lower bound" to the dielectric loss for wavelengths $2.7-4.0$ mm, which was lower than MW's value at 3 mm by a factor of ~ 2, but because it is a lower bound it does not dispute the values of MW.

[28] More recently, *Zhang et al.* [2001] used time domain spectroscopy to measure the optical constants in the terahertz region, wavelengths $0.3-1.2$ mm, at five temperatures between 239 and 264 K. Their values of m_{im} agree well with an extrapolation of MW's data to shorter wavelengths.

[29] *Mätzler* [2006] showed that a theoretical temperature-dependent formula for m_{im}, with empirically determined coefficients, would accurately fit the measurements of MW, *Zhang et al.* [2001], *Matsuoka et al.* [1996], and *Mishima et al.* [1983] for wavelengths $0.3-100$ mm and temperatures $190-258$ K. We accept Mätzler's formula, computed for $T = 266$ K. We use it out to the longwave limit of MW's extrapolation, $\lambda = 2$ m, where it agrees with values of *Johari and Charette* [1975] that were used by W84. At the shortwave end, we interpolate between Zhang et al.'s measurement at $\lambda = 300$ μm and the temperature-adjusted, far-infrared value of *Curtis et al.* [2005] at $\lambda = 75$ μm, as described in section 4.2. Between 200 and 300 μm our interpolated m_{im} parallels that measured by *Whalley and Labbé* [1969] at 200 K, shown in Figure 6 of W84.

[30] The temperature dependence dk_a/dT increases with wavelength in the microwave region, and the position of the minimum near $\lambda = 100$ mm shifts to longer wavelength with decreasing temperature. In the revised compilation (Figure 6) we show the values only for a single temperature, 266 K, just to complete our description of the absorption spectrum. Researchers requiring optical constants in the microwave for other temperatures should consult *Mätzler* [2006] and use his formulas directly (a link to Mätzler's book chapter is on our website). For our compilation we have chosen wavelengths such that an interpolation (log m_{im}

Figure 6. Imaginary part of the complex index of refraction of ice in the microwave and radio wave region; comparison of the new compilation to that of *Warren* [1984].

versus log λ) between adjacent points deviates from MW's formula by at most 1%.

[31] The microwave properties of ice and snow, including the effect of salt in sea ice, are reviewed by *Mätzler* [1998].

6. Computation of Real Index

[32] The spectra of $m_{re}(\lambda)$ and $m_{im}(\lambda)$ are related by KK relations, as described by W84. We follow the procedure of W84, carrying out a KK analysis of the revised spectrum of m_{im} to compute the spectrum of the real part of the refractive index, m_{re}. The real index is known accurately from experiments in the two spectral regions of minimum absorption, visible and microwave; so we force the KK analysis to agree with the measurements at two chosen wavelengths. As in W84, we scale the strength of the X-ray band to obtain the correct visible m_{re} at $\lambda = 589.3$ nm, and we scale the far-IR bands to obtain the correct microwave m_{re} at $\lambda = 200$ mm. Only small adjustments were needed. The computed m_{re} spectrum is plotted in Figure 7. It differs substantially from the W84 values in the far IR, 30–200 μm. Elsewhere it differs from the W84 values by at most 2%.

7. Uncertainty of the Compilation

[33] Uncertainty estimates for the absorption coefficient are available from the original measurements, and additional uncertainty is introduced where we extrapolate the temperature dependence to 266 K. Our estimates of the uncertainty in m_{im} are shown in Figures 8 and 9; they are based on the following considerations.

[34] Uncertainty of k_a for 350–600 nm is shown by *Warren et al.* [2006, Figure 7]. We accept those error estimates for 390–600 nm, but as indicated in section 2,

the absorption by ice for 350–390 nm is extremely weak, and the experimental absorption was probably dominated by impurities. For the region 200–350 nm we, therefore, have not determined a lower limit to m_{im}. The upper bound on m_{im} is taken from the value at 350 nm and extrapolated back to 200 nm. This gives a large relative error in Figure 8 because the absolute value of m_{im} is extremely small here. For 0.6–1.4 μm, error bars are given by *Grenfell and Perovich* [1981, Table 1] and are either 8% or 10%, as shown by the three short horizontal bars in Figure 8.

[35] For 1.4–7.8 μm (except in the 3-μm band), error bars are given by *Gosse et al.* [1995, Table 1]; they are plotted as points in Figure 8. For 2.9–3.4 μm, error bars are shown by *Schaaf and Williams* [1973, Figure 4a]; the corresponding numerical values are given by *Schaaf* [1973, Table 3]. Schaaf estimated the uncertainty in two different ways, but the results were similar; at each wavelength we plot the larger of his two estimates.

[36] For 7.8–10.3 μm the uncertainty is taken as the difference in Figure 4 between our compilation and the value of *Schaaf and Williams* [1973] or the value of *Toon et al.* [1994], whichever gives the larger difference. For 10.3–26 μm the error bars again come from *Schaaf* [1973, Table 3].

[37] For 26–200 μm the uncertainty in our temperature extrapolation greatly exceeds the experimental error of *Curtis et al.* [2005] at the reported temperatures. We give a conservative estimate of the relative uncertainty as

$$\left| \frac{m_{im}(266) - m_{im}(176)}{m_{im}(266)} \right|,$$

where $m_{im}(176)$ is the reported value at 176 K and $m_{im}(266)$ is our extrapolation to 266 K.
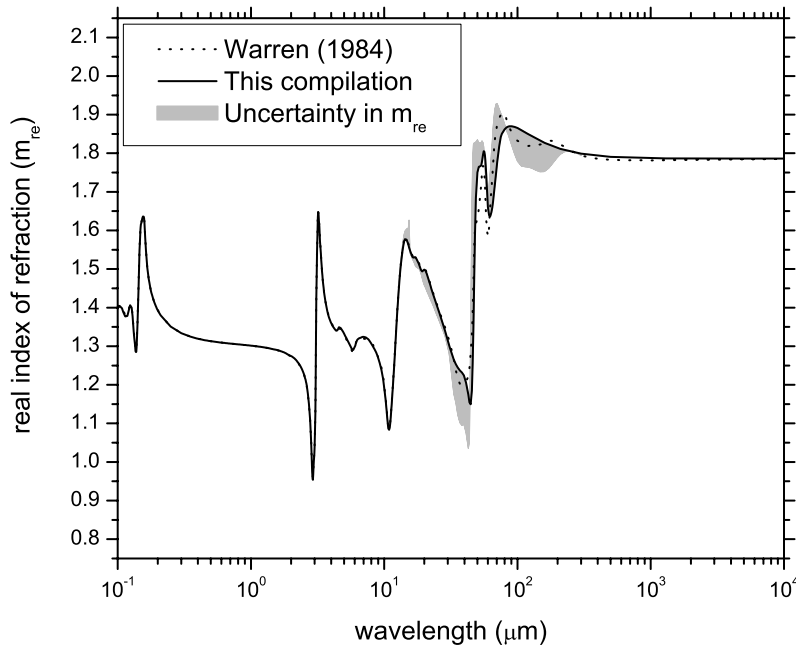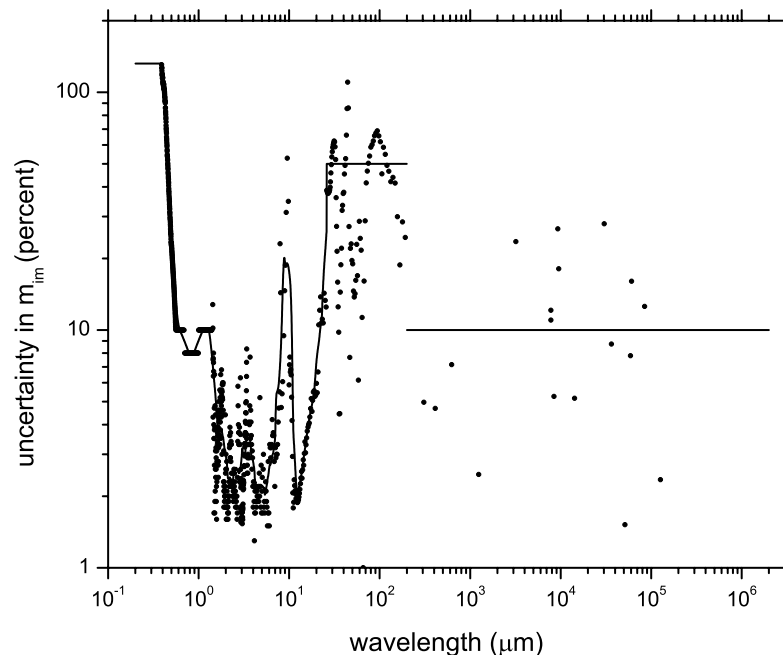
Figure 7. Real part of the complex index of refraction of ice; comparison of the new compilation to that of *Warren* [1984]. Uncertainty is indicated by the shading.

[38] For wavelengths $200-2$ m, we plot either the reported experimental uncertainty or the discrepancy between the two sources, whichever is larger. The discrepancy between *Mätzler and Wegmüller* [1987] and *Matsuoka et al.* [1996] is small; the two data sets were plotted together by *Zhang et al.* [2001, Figure 2b].

[39] In Figure 8 we also draw a smooth curve through the uncertainty estimates to show representative values in broad bands. For the far-infrared and microwave regions we just draw horizontal lines showing 50% and 10% uncertainty,

respectively, which we take to be representative uncertainties for these regions.

[40] For the real part of the refractive index, the uncertainty is significant only in the far infrared, $30-200$ μm, where m_{im} is large and uncertain because of our temperature extrapolation. *Curtis et al.* [2005] obtained both m_{im} and m_{re} at each of their temperatures using KK analysis. In Figure 7 we use shading to display the difference between their m_{re} for 176 K and our m_{re} for 266 K; this is an indication of the uncertainty in our compilation of m_{re}. Figure 9 displays the

Figure 8. Estimated percent uncertainty of m_{im}.
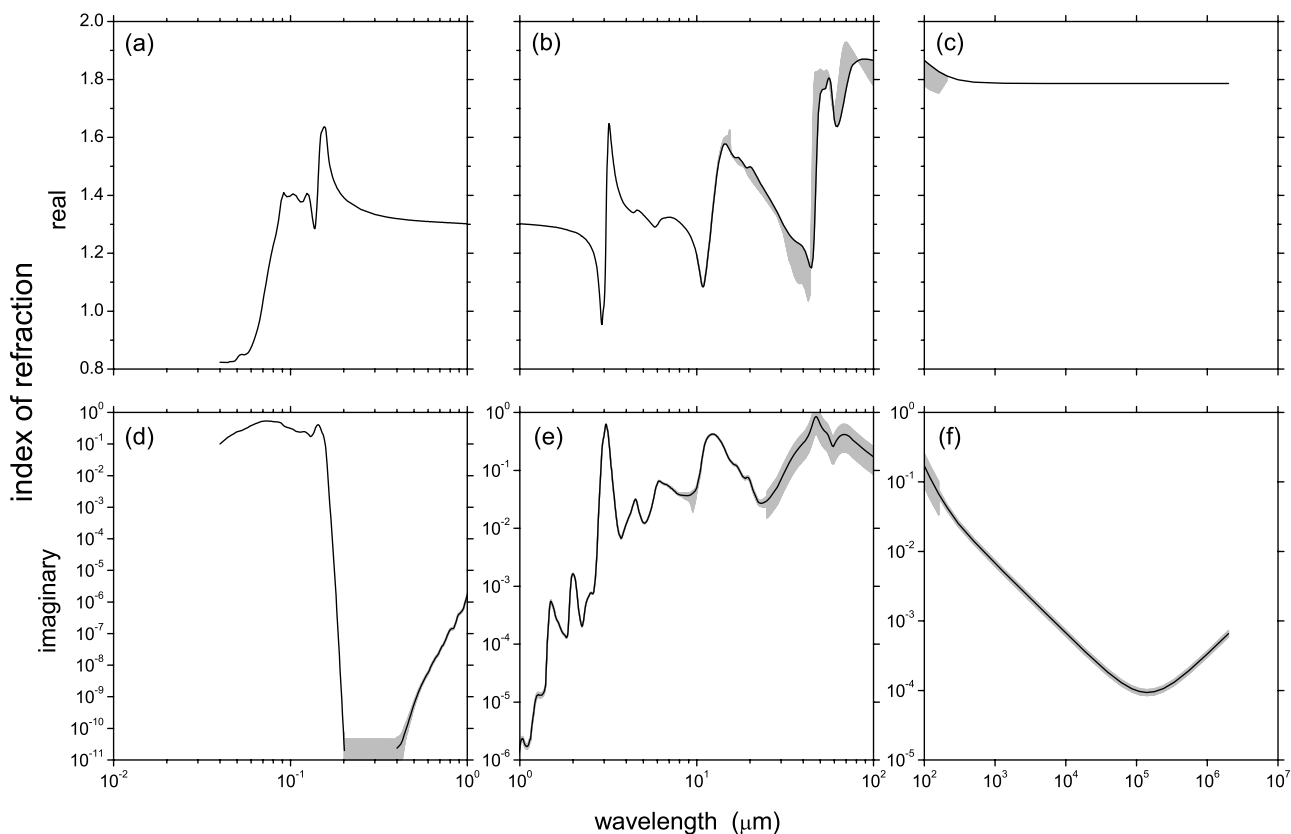
Figure 9. Compilation of the (a)–(c) real and (d)–(f) imaginary parts of the complex index of refraction of ice Ih at temperature 266 K. Uncertainty is indicated by the shading.

entire spectrum of the complex index of refraction, with shading to indicate the error bars.

8. Conclusions

[41] The new compilation of m_{re} and m_{im} is available at http://www.atmos.washington.edu/ice_optical_constants. The compilation of m_{im} deviates significantly from W84 in several regions. The largest relative changes, by far, are in the visible and near ultraviolet. These changes will have no effect on the computed radiative properties of clouds and minor effects on computations of snow albedo but will be significant for computation of photochemical fluxes in snow [*Wolff et al.*, 2002] and of ice thickness on the ocean of "Snowball Earth" [*Warren et al.*, 2002].

[42] The new values in the near infrared, 1.4–5 μm, are larger by a factor of 2 at some wavelengths and smaller by a factor of 2 at other wavelengths. These changes are important for remote sensing of ice clouds, for distinguishing ice clouds from water clouds, and for distinguishing clouds from snow by satellites using reflection of near-infrared solar radiation. The absorption coefficient for 7–10 μm is lower than in W84 by 30% in places; this region is near the peak of Earth's emission spectrum and also includes an important absorption band of ozone.

[43] For 15–30 μm (i.e., between the 12-μm libration band and the first lattice vibration), the absorption coefficient apparently depends strongly on temperature. This region is significant for absorption and emission of long-

wave radiation by ice clouds. For atmospheric transmission it is called the "dirty window," where the opacity of water vapor above cirrus clouds is significant and variable.

[44] The far-IR bands, also important for radiative cooling to space by ice clouds, have been revised significantly. The 45-μm peak is stronger than in the 1984 compilation; the 65-μm peak is weaker and shifted to a longer wavelength (∼70 μm).

[45] In the microwave region the compilation of W84 has long been obsolete, as it was superseded already in 1987 by MW. The MW values are lower than W84 by a factor of 5 for centimeter wavelengths, with significance for interpretation of microwave remote sensing.

[46] New measurements of absorption spectrum of ice near the melting point would be desirable in two regions of the infrared: (1) 8–10 μm, ideally establishing the temperature dependence of absorption between 200 and 273 K, and (2) 15–300 μm. The data of SW for 15–33 μm are at suitably high temperature (266 K) but are noisy; they require confirmation. For 33–200 μm the highest temperature for which accurate measurements are available is 176 K, and for 200–300 μm it is 200 K.

References

Ackermann, M., et al. (2006), Optical properties of deep glacial ice at the South Pole, *J. Geophys. Res.*, *111*, D13203, doi:10.1029/2005JD006687.

Askebjer, P., et al. (1997), Optical properties of deep ice at the South Pole: Absorption, *Appl. Opt.*, *36*, 4168–4180, doi:10.1364/AO.36.004168.

Bertie, J. E., and S. M. Jacobs (1977), Far-infrared absorption by ices Ih and Ic at 4.3°K and the powder diffraction pattern of ice Ic, *J. Chem. Phys.*, *67*, 2445–2448, doi:10.1063/1.435218.

Bertie, J. E., and E. Whalley (1967), Optical spectra of orientationally disordered crystals: II. Infrared spectrum of ice Ih and ice Ic from 360 to 50 cm^{-1}, *J. Chem. Phys.*, *46*, 1271–1284, doi:10.1063/1.1840845.

Bertie, J. E., H. J. Labbé, and E. Whalley (1969), Absorptivity of ice I in the range 4000–30 cm^{-1}, *J. Chem. Phys.*, *50*, 4501–4520, doi:10.1063/1.1670922.

Curtis, D. B., B. Rajaram, O. B. Toon, and M. A. Tolbert (2005), Measurement of the temperature-dependent optical constants of water ice in the 15–200 μm range, *Appl. Opt.*, *44*, 4102–4118, doi:10.1364/AO.44.004102.

Gosse, S., D. Labrie, and P. Chylek (1995), Refractive index of ice in the 1.4–7.8-μm spectral range, *Appl. Opt.*, *34*, 6582–6586.

Grenfell, T. C., and D. K. Perovich (1981), Radiation absorption coefficients of polycrystalline ice from 400 to 1400 nm, *J. Geophys. Res.*, *86*, 7447–7450, doi:10.1029/JC086iC08p07447.

Grundy, W. M., and B. Schmitt (1998), The temperature-dependent near-infrared absorption spectrum of hexagonal H$_2$O ice, *J. Geophys. Res.*, *103*, 25,809–25,822, doi:10.1029/98JE00738.

He, Y. D., and P. B. Price (1998), Remote sensing of dust in deep ice at the South Pole, *J. Geophys. Res.*, *103*, 17,041–17,056, doi:10.1029/98JD01643.

Johari, G. P., and P. A. Charette (1975), The permittivity and attenuation in polycrystalline and single-crystal ice Ih at 35 and 60 MHz, *J. Glaciol.*, *14*, 293–303.

Johnson, B. R., and S. K. Atreya (1996), Feasibility of determining the composition of planetary ices by far infrared observations: Application to Martian cloud and surface ices, *Icarus*, *119*, 405–426, doi:10.1006/icar.1996.0027.

Koh, G. (1997), Dielectric properties of ice at millimeter wavelengths, *Geophys. Res. Lett.*, *24*, 2311–2313, doi:10.1029/97GL02272.

Kou, L., D. Labrie, and P. Chylek (1993), Refractive indices of water and ice in the 0.65- to 2.5-μm spectral range, *Appl. Opt.*, *32*, 3531–3540.

Maldoni, M. M., R. G. Smith, G. Robinson, and V. L. Rookyard (1998), A study of the 2.5–25 μm spectrum of H$_2$O ice, *Mon. Not. R. Astron. Soc.*, *298*, 251–258, doi:10.1046/j.1365-8711.1998.01621.x.

Matsuoka, T., S. Fujita, and S. Mae (1996), Effect of temperature on dielectric properties of ice in the range 5–39 GHz, *J. Appl. Phys.*, *80*, 5884–5890, doi:10.1063/1.363582.

Mätzler, C. (1998), Microwave properties of ice and snow, in *Solar System Ices*, edited by B. Schmitt, C. De Bergh, and M. Festou, pp. 241–257, Kluwer, Dordrecht, Netherlands.

Mätzler, C. (2006), Microwave dielectric properties of ice, in *Thermal Microwave Radiation—Applications for Remote Sensing, Electromagn, Waves Ser.*, vol. 52, edited by C. Mätzler et al., chap. 5, 455–462, Inst. Eng. Technol., Stevenage, U. K.

Mätzler, C., and U. Wegmüller (1987), Dielectric properties of fresh-water ice at microwave frequencies, *J. Phys. D Appl. Phys.*, *20*, 1623–1630, doi:10.1088/0022-3727/20/12/013. (Correction, *J. Phys. D. Appl. Phys.*, *21*, 1660, doi:10.1088/0022-3727/21/11/522, 1988.)

Minton, A. (1971), The far-ultraviolet spectrum of ice, *J. Phys. Chem.*, *75*, 1162–1164, doi:10.1021/j100678a024.

Mishima, O., D. D. Klug, and E. Whalley (1983), The far-infrared spectrum of ice Ih in the range 8–25 cm^{-1}: Sound waves and difference bands, with application to Saturn's rings, *J. Chem. Phys.*, *78*, 6399–6404, doi:10.1063/1.444700.

Moore, M. H., and R. L. Hudson (1992), Far-infrared spectral studies of phase changes in water ice induced by proton irradiation, *Astrophys. J.*, *401*, 353–360, doi:10.1086/172065.

Ockman, N. (1957), The infrared-spectra and Raman-spectra of single crystals of ordinary ice, Ph.D. thesis, 171 pp., Univ. of Michigan, Ann Arbor.

Ockman, N. (1958), The infra-red and Raman spectra of ice, *Adv. Phys.*, *7*, 199–220.

Perovich, D. K., and J. W. Govoni (1991), Absorption coefficients of ice from 250 to 400 nm, *Geophys. Res. Lett.*, *18*, 1233–1235, doi:10.1029/91GL01642.

Rajaram, B., D. L. Glandorf, D. B. Curtis, M. A. Tolbert, O. B. Toon, and N. Ockman (2001), Temperature-dependent optical constants of water ice in the near infrared: New results and critical review of the available measurements, *Appl. Opt.*, *40*, 4449–4462, doi:10.1364/AO.40.004449.

Schaaf, J. W. (1973), The infrared reflectance of ice I, Ph.D. thesis, 173 pp., Kansas State Univ., Manhattan.

Schaaf, J. W., and D. Williams (1973), Optical constants of ice in the infrared, *J. Opt. Soc. Am.*, *63*, 726–732.

Schmitt, B., E. Quirico, F. Trotta, and W. M. Grundy (1998), Optical properties of ices from UV to infrared, in *Solar System Ices*, edited by B. Schmitt, C. de Bergh, and M. Festou, pp. 199–240, Kluwer, Dordrecht, Netherlands.

Toon, O. B., M. A. Tolbert, B. G. Koehler, A. M. Middlebrook, and J. Jordan (1994), Infrared optical constants of H$_2$O ice, amorphous nitric acid solutions, and nitric acid hydrates, *J. Geophys. Res.*, *99*, 25,631–25,654, doi:10.1029/94JD02388.

Tsujimoto, S., A. Konishi, and T. Kunitomo (1982), Optical constants and thermal radiative properties of H$_2$O cryodeposits, *Cryogenics*, *22*, 603–607, doi:10.1016/0011-2275(82)90009-1.

Warren, S. G. (1984), Optical constants of ice from the ultraviolet to the microwave, *Appl. Opt.*, *23*, 1206–1225.

Warren, S. G., R. E. Brandt, T. C. Grenfell, and C. P. McKay (2002), Snowball Earth: Ice thickness on the tropical ocean, *J. Geophys. Res.*, *107*(C10), 3167, doi:10.1029/2001JC001123.

Warren, S. G., R. E. Brandt, and T. C. Grenfell (2006), Visible and near-ultraviolet absorption spectrum of ice from transmission of solar radiation into snow, *Appl. Opt.*, *45*, 5320–5334, doi:10.1364/AO.45.005320.

Whalley, E., and H. J. Labbé (1969), Optical spectra of orientationally disordered crystals: III. Infrared spectra of the sound waves, *J. Chem. Phys.*, *51*, 3120–3127, doi:10.1063/1.1672464.

Wieliczka, D. M., S. Weng, and M. R. Querry (1989), Wedge shaped cell for highly absorbent liquids: Infrared optical constants of water, *Appl. Opt.*, *28*, 1714–1719.

Wolff, E. W., A. E. Jones, T. J. Martin, and T. C. Grenfell (2002), Modelling photochemical NO$_x$ production and nitrate loss in the upper snowpack of Antarctica, *Geophys. Res. Lett.*, *29*(20), 1944, doi:10.1029/2002GL015823.

Woschnagg, K., and P. B. Price (2001), Temperature dependence of absorption in ice at 532 nm, *Appl. Opt.*, *40*, 2496–2500, doi:10.1364/AO.40.002496.

Zhang, C., K.-S. Lee, X.-C. Zhang, X. Wei, and Y. R. Shen (2001), Optical constants of ice Ih crystal at terahertz frequencies, *Appl. Phys. Lett.*, *79*, 491–493, doi:10.1063/1.1386401.

Zimmermann, R., and G. C. Pimentel (1962), The infrared spectrum of ice: Temperature dependence of the hydrogen bond potential function, in *Advances in Molecular Spectroscopy*, edited by A. Mangini, pp. 726–737, Macmillan, New York.

————————————

R. E. Brandt and S. G. Warren, Department of Atmospheric Sciences, University of Washington, Seattle, WA 98195-1640, USA. (brandt@atmos.washington.edu; sgw@atmos.washington.edu)